FEATURE ARTICLE

High-Performance Organic Field-Effect Transistors: Molecular Design, Device Fabrication, and Physical Properties

Chong-an Di,[†,‡] Gui Yu,*[,†] Yunqi Liu,*[,†] and Daoben Zhu[†]

Beijing National Laboratory for Molecular Sciences, and Key Laboratory of Organic Solids, Institute of Chemistry, Chinese Academy of Sciences. Beijing 100080, P. R. China, Graduate School of Chinese Academy of Sciences, Beijing 100039, P. R. China

Received: March 4, 2007; In Final Form: August 24, 2007

In the past decade, tremendous progress has been made in organic field-effect transistors (OFETs). Their real applications require further development of device performance. OFETs consist of organic semiconductors, dielectric layers, and electrodes. Organic semiconductors play a key role in determining the device characteristics. The properties of the organic semiconductors, such as molecular structure and packing, as well as molecular energy levels, can be properly controlled by molecular design. Therefore, we designed and synthesized a series of organic molecules. The synthesized organic semiconductors exhibit excellent field-effect properties due to strong intermolecular interactions and proper molecular energy levels. Meanwhile, the influence of the device fabrication process, organic semiconductor/dielectric layer interface, and organic layer/electrode contact on the device performance was investigated. A deep understanding of these factors is helpful to improve field-effect properties. Furthermore, single-crystal field-effect transistors are highlighted because the single-crystal-based FETs can provide an accurate conducting mechanism of organic semiconductors and higher device performance as compared with thin film FETs.

1. Introduction

Organic thin films have been widely investigated as active layers in optoelectronic devices.[1−5] Compared with their inorganic counterparts, organic optoelectronic devices possess many unique advantages, such as light weight, low cost, flexibility, and low-temperature device fabrication. Recently, organic field-effect transistors (OFETs) have received significant research interest, and remarkable progress has been made. Although it could be difficult for OFETs to fully replace silicon technology in the field, where high performance and excellent stability are necessary, they hold promise for application in integrated circuits for large-area, flexible, and ultralow-cost electronics, such as radio frequency identification (RFID) tags, smart cards, and organic active matrix displays. More recently, studies have demonstrated that numerous organic materials exhibit carrier mobilities comparable to hydrogenated amorphous silicon (a-Si:H).[6−14] The stability of OFETs has also experienced a dramatic improvement.[15] In addition, several solution-processable organic semiconductors and economical fabrication techniques have been developed to decrease the cost of OFETs.[16−19]

A typical OFET is composed of a gate electrode, dielectric layer, organic semiconductor layer, and source−drain (S−D) electrodes (Figure 1). The dielectric layers are either inorganic dielectric materials or insulating organic polymers. The organic semiconductor is the core element of an OFET. It determines the charge carrier transport as well as the charge carrier injection. Inorganic semiconductors are classified into p-type or n-type materials, depending on the nature of the controlled dopant. Different from inorganic materials, organic semiconductor materials can be classified as p-type or n-type according to which type of charge carrier is more efficiently transported through the material.[20] In fact, all organic semiconductors allow hole and electron transport; however, the carrier transport mobility is difficult to measure accurately. The organic semiconductor category is thus determined by the operation model of corresponding devices. For OFETs, both the carrier transport and the carrier injection influence the device operation model. In other words, aside from the properties of the organic materials, both the work function of S−D electrodes and the dielectric properties of the insulating layer could influence the device operation model. As a result, it is not appropriate to define p- or n-type semiconductors, but rather p- or n-channel transistors. When holes are preferentially injected into the organic active layer, they accumulate at the organic/dielectric layer interface and transport through the channel; thus, the device exhibits p-type operation. Most reported OFETs are p-type. In contrast, if the electrons are injected into the semiconductors and transport through the active channel, the OFETs can be characterized as n-type. Generally, for both p-type and n-type OFETs, if only one kind of carrier (hole or electron) is preferentially injected and transported, the devices exhibit unipolar characteristics. When both holes and electrons can be injected and transport in the same device, the devices show ambipolar characteristics. Compared with unipolar devices, ambipolar OFETs could realize both the p-type and n-type operation in the same device, and they possess many unique

* To whom correspondence should be addressed. E-mails: (G.Y.) yugui@mail.iccas.ac.cn, (Y.L.) liuyq@mail.iccas.ac.cn.
† Institute of Chemistry.
‡ Graduate School of Chinese Academy of Sciences.

10.1021/jp071753b CCC: $37.00
Published on Web 12/05/2007

Chong-an Di was born in Shandong, China, in 1981. He received his B.S. degree in chemistry from Qufu Normal University (2003). Since September 2003, he has been a Ph.D. student at the Institute of Chemistry, Chinese Academy of Sciences (CAS). His research interest includes fabrication, characterization, and optimization of organic field-effect transistors and organic light-emitting diodes.

Gui Yu was born in Changchun, China, in 1965. He graduated from Jiling University in 1988 and received his M.S. (1993) and Ph.D. (1997) degrees from Changchun Institute of Physics, Chinese Academy of Sciences. After completing his Ph.D., he went to the Institute of Chemistry, CAS, as a postdoctorate. He was appointed to the position of Associate Professor in 1999 and promoted to Professor in 2007. His research interest focuses on synthesis, structures, electronic and optical properties, and theoretical investigation of novel organic semiconductors.

Yunqi Liu was born on April 1, 1949. He graduated from the Department of Chemistry, Nanjing University, in 1975 and received a doctorate from Tokyo Institute of Technology, Japan, in 1991. Presently, he is a professor of the Institute of Chemistry, CAS. His research interests include molecular materials and devices.

Daoben Zhu was born on August 20, 1942. He finished his graduate courses at the East China University of Science and Technology in 1968. Currently, he is a professor and the Director of the Organic Solids Laboratory of the Institute of Chemistry, CAS. He was selected as an academician of CAS in 1997. His research interests include molecular materials and devices.

characteristics, as listed in previous reviews.[21] According to different preparation sequences of the S−D electrodes and organic semiconductor layer, OFETs are fabricated in either the top or bottom S−D contact geometry (Figure 1a and b). In the top contact configuration, the organic layer is located on a dielectric surface, and the S−D electrodes are deposited onto the top of the organic layer through a shadow mask. For devices with top contact geometry, excellent electrode/organic layer contact and high device performance can be obtained. In bottom contact devices, the S−D electrodes are sandwiched between the gate dielectric layer and the organic semiconductor layer. Bottom contact S−D electrodes can be prepared on the dielectric layer using photolithographic techniques. Compared with top contact geometry, the bottom contact configuration is a more feasible geometry for many practical applications. Unfortunately, bottom contact devices usually suffer from lower device performance due to the poor contact. For the above-mentioned two configurations, both the dielectric layer and the gate electrode are fabricated before the organic layer deposition. These configurations correspond to the bottom-gate geometry. The bottom-gate geometry is the most used device structure. On the other hand, OFETs can also be constructed in the top-gate configuration, where the gate electrode is the last device element deposited. With this geometry, the organic active layer can be well-encapsulated by the following deposition of the dielectric layer and gate electrode. For single-crystal FETs, the top-gate geometry ensures good dielectric/single-crystal contact.

The accumulation model is the most frequently applied method to describe OFETs. In OFETs with p-type semiconductors, when no voltage is applied to the gate electrode, only small currents flow between the source and drain electrodes due to low carrier density in the organic semiconductor layer, and the device is in the "off" state. When the negative gate voltage is biased, a conductive channel forms as a result of the accumulation of holes at the organic layer/dielectric layer interface. Hence, hole injection and transport occur with a source−drain voltage. This state corresponds to the "on" state. It should be noted that deep traps at the organic layer/dielectric layer interface could confine some induced carriers. As a result, a gate voltage (V_G) larger than the threshold voltage (V_T) is necessary to turn the transistor to the "on" state. For $V_G > V_T$, when a source−drain voltage (V_{DS}) is applied, the holes are injected from the source electrode and transport through the conductive channel to the drain electrode. In the small S−D voltage region, the current increases linearly with S−D voltage and follows Ohm's law.

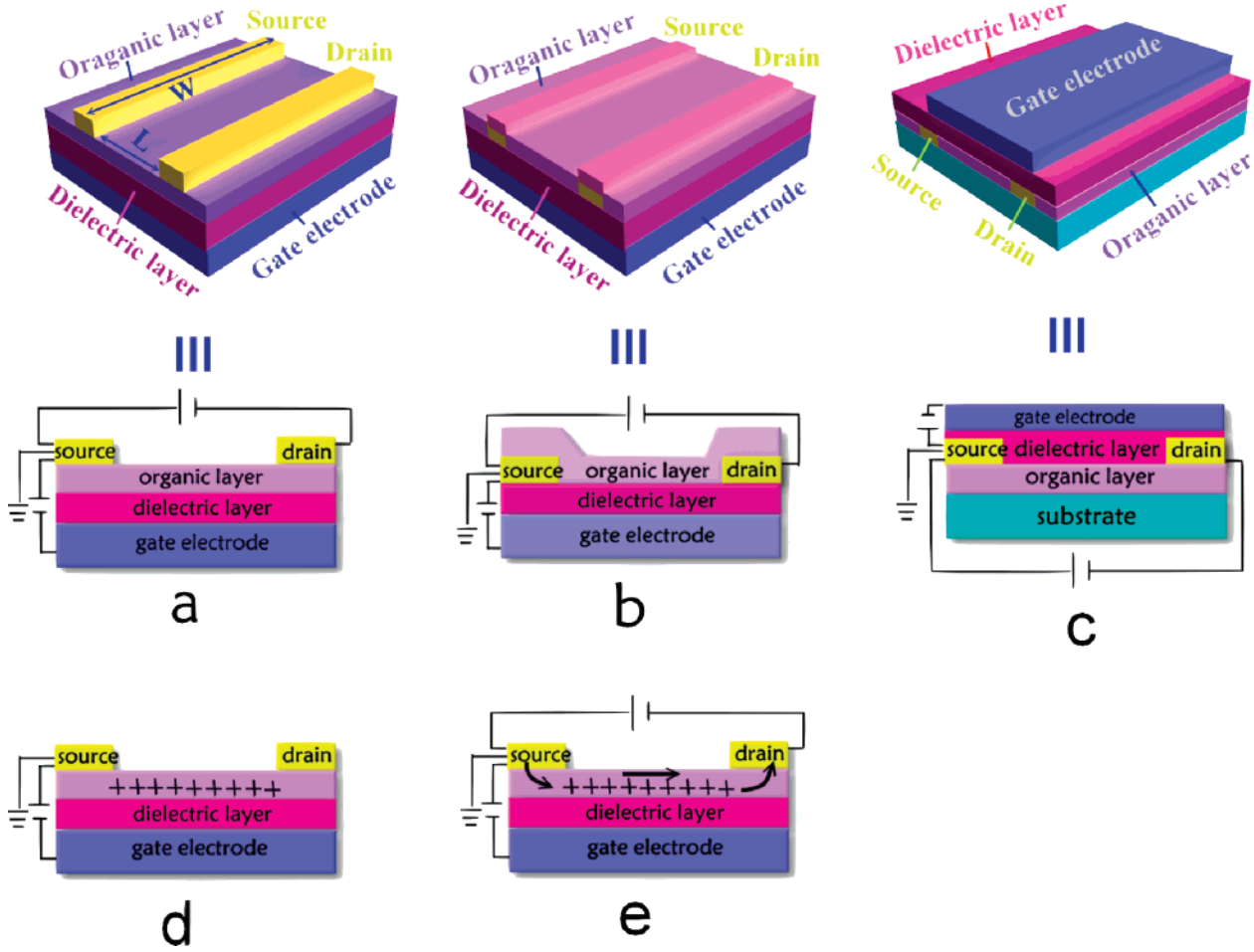

Figure 1. Schematic diagram of the device configuration and operation mechanism: (a) top-contact configuration, (b) bottom-contact configuration, (c) top-gate structure, (d) formation of conductive channel resulting from hole accumulation at the organic layer/dielectric layer interface when the gate voltage is biased, and (e) the carrier injection from the source electrode and transport through the channel to the drain electrode.

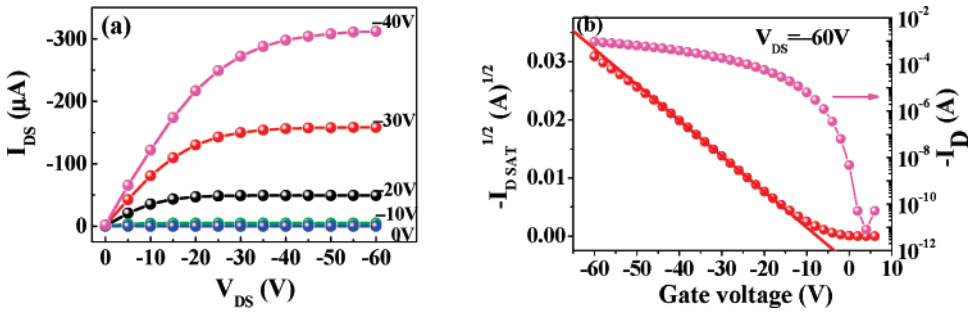

Figure 2. (a) Output and (b) transfer characteristics of pentacene-based OFETs with bottom contact configuration. The channel length and width are 10 μm and 1.4 mm, respectively.

When a larger source−drain voltage ($V_{DS} \geq V_G - V_T$) is biased, the channel is "pinched off" due to the depletion of carriers near the drain electrode. It in turn leads to a saturated source−drain current, which is independent of the source−drain voltage. For n-type OFETs, the positive source−drain voltages and gate voltages are biased; therefore, electrons are injected into the n-type active layer, accumulate in the conductive channel, and transport to the drain electrode. Figure 2 shows the output and transfer characteristics of an OFET based on pentacene (p-type). As seen in Figure 2a (output curve), when the gate electrode is negatively biased, the drain current (I_D) increases with gate voltage (V_G). When the V_G is maintained, I_D increases for low S−D voltage (V_{DS}) and then saturates ($I_{D,sat}$) at larger V_{DS}. These results indicate that the pentacene-based FETs are unipolar p-type devices working in accumulation mode. All the key parameters were extracted from the transfer characteristic curve at a constant drain−source voltage (Figure 2b). The field effect mobility (μ), on/off ratio, and threshold voltage are the most important parameters. The field effect mobility is the majority carrier mobility of the semiconductor material derived through transfer curve measurement of the fabricated device. This value can be extracted by using the following equations in the saturation regime (1) or the linear region (2), respectively,

$$I_D = \mu C \frac{W}{L}\left[\frac{(V_G - V_T)^2}{2}\right] \quad (1)$$

$$I_D = \mu C \frac{W}{L}\left[(V_G - V_T)V_D - \frac{V_D^2}{2}\right] \quad (2)$$

where W and L are the channel width and length, respectively, C is the gate dielectric capacitance per unit area (10 nF/cm^2), and V_T is the threshold voltage. On/off ratio is the maximum I_{DS}(on) value divided by the minimum I_{DS}(off) value, which depends strongly on the maximum gate voltage biased. The threshold voltage is the minimum gate voltage required to induce the channel. Analysis of Figure 2 indicated a field effect mobility of 0.54 cm^2 V^{-1} s^{-1}, an on/off current ratio of 10^7 at the drain voltage of -60 V, and a threshold voltage of -7.5 V (deduced from the intercept at $y = 0$ of the $(|I_{D,sat}|)^{1/2}$ vs V_G plot). This device performance is comparable to that of the inorganic device based on the hydrogenated amorphous silicon (a-Si:H).

Fabrication of OFETs with high performance, excellent stability, and low cost is a preferred research area. Nowadays, most research is focused on following the parts: (a) Molecular design of new organic semiconductors and the application of existing materials that have never been used in OFETs. It should be noted that a organic semiconductor should have a high carrier mobility, excellent stability, and low cost for both the material synthesis and film fabrication. (b) Improvement of device fabrication techniques. The film deposition condition, the organic layer/dielectric layer interface, and the electrode/organic layer contact play important roles in determining the device performance. Therefore, optimizing the device's configuration could dramatically enhance device performance without changing the organic semiconductors. Studying single-crystal FETs is helpful to achieve high device performance and to deeply understand conducting the mechanism of the organic semiconductors. (c) Lowering the device cost and building flexible devices. These unique characteristics are of great importance for OFETs when compared with their inorganic counterparts. All parts of the device, including electrodes, organic layer, substrate, and dielectric layer, could be replaced by materials with low fabrication cost, flexible materials, or both. (d) Exploration of OFET applications. It has been demonstrated that OFETs have numerous potential applications, such as RFID, organic active matrix display, memory devices, electronic paper, sensors, and electronic skins. These applications can act as drivers for the further development of OFETs. In this article, we summarize our recent results in molecular design, device fabrication, and optimization toward high field-effect performance.

2. Molecular Design

The organic semiconductor is the core element of OFETs. Therefore, the development of excellent organic semiconductors is a key issue for the fabrication of high-performance devices. Mobility >1 cm^2/V s has been obtained for many OFETs.[22−24] This device performance could be adequate for some applications, such as RFID and an active pixel drive circuit for liquid crystal displays. However, the conducting mechanism of organic semiconductors still remains unclear. As for inorganic semiconductors, the inorganic atoms are held together with strong covalent bonds, and the charge carriers move as highly delocalized plane waves in wide bands with high mobility. For organic semiconductors, the weak van der Waals interaction between the organic molecules is responsible for the carrier transport.[25] Therefore, different conducting mechanisms are proposed, including the thermally activated hopping mechanism, the bandlike mechanism, and multiple trapping and release (MTR).[25−29] According to the previous mechanism, the carrier transport occurs via polaron hopping (the deformation of the lattice around the electron or hole) between localized states. Hopping is assisted by phonons, and the charge mobility increases with increasing temperature. However, the hopping model is generally accepted for disordered materials. It has been claimed that the simple thermally activated hopping mechanism can be excluded as a transport mechanism for organic single crystals. This conclusion was drawn from the increased mobility of organic single crystals with decreasing temperature, which was investigated by time-of-flight and time-resolved terahertz pulse spectroscopy as well as field-effect transistor measurement on high-purity crystals.[21,30−32] Therefore, bandlike transport of delocalized carriers is suggested instead of hopping transport. Unfortunately, the model is still unsatisfactory. More recently, intermolecular electronic coupling modulated by thermal motion and the polarizability of the gate dielectric layer (in organic single-crystal FETs) were believed to contribute to the localization of charge carriers in a highly ordered system.[33,34] Another model, the MTR model, assumes that charge transport occurs in a delocalized band, while it is limited by the distribution of traps near the band.[26−28] For polycrystalline thin films, the trapped state could exist in grain boundaries rather than be uniformly distributed throughout the film. Consequently, traps at the grain boundaries in polycrystalline film should be responsible for the temperature-independent mobility at low temperature. Together with the above-mentioned charge transport mechanism, we note that regardless of what the ultimate transport mechanism is, strengthened intermolecular interaction and overlap are preferable for effective carrier transport. Additionally, the energy levels and gaps, which influence carrier injection and semiconductor stability, play important roles in determining the device performance. As a unique characteristic of the organic semiconductors, the molecular packing, energy level and other physical properties can be controlled by the molecular design. Therefore, we designed and synthesized a series of organic semiconductors suitable for OFET applications.

2.1. Thiophene Derivatives. To achieve high field-effect performance, strong intermolecular interactions, proper energy levels, and highly ordered films are necessary. Pentacene is one of the most outstanding organic field-effect materials. Its excellent field-effect properties result from the following characteristics. First, the extended π system of the high acene enhances the intermolecular overlap of $\pi-\pi$ systems in the solid state, in turn leading to effective carrier transport.[35] Second, pentacene possesses a proper HOMO energy level, which matches the work function of source−drain electrodes and facilitates hole injection.[36] Furthermore, the excellent polycrystalline-film-forming property leads to fewer boundary-induced traps. Unfortunately, pentacene suffers from the disadvantages of oxidative instability and strong absorbance throughout the visible spectrum.[37] Thiophene-based materials exhibit a variety of intra- and intermolecular interaction, such as van der Waals interactions, weak hydrogen bonds, $\pi-\pi$ stacking, and sulfur−sulfur interactions.[38,39] As a result, thiophene derivatives are a promising class of organic semiconductors for OFETs. Recently, it has been demonstrated that many OFETs based on thiophene derivatives exhibited both high performance and excellent stability.[40,41]

Oligothiophenes have been widely used in organic FETs. However, they might twist from planarity, thus disrupting the conjugated structure. The linearly condensed thiophenes give the most extended π-conjugation and the highest planarity. In addition, efficient intermolecular S−S interactions could contribute to the carrier transport. Dithieno[2,3-*d*:2′,3′-*d*′]thieno-[3,2-*b*:4,5-*b*′]dithiophene (pentathienoacene, PTA, compound **2**, see Figure 3) has a molecular shape and crystal packing geometry similar to those of pentacene.[36] The energy gap of

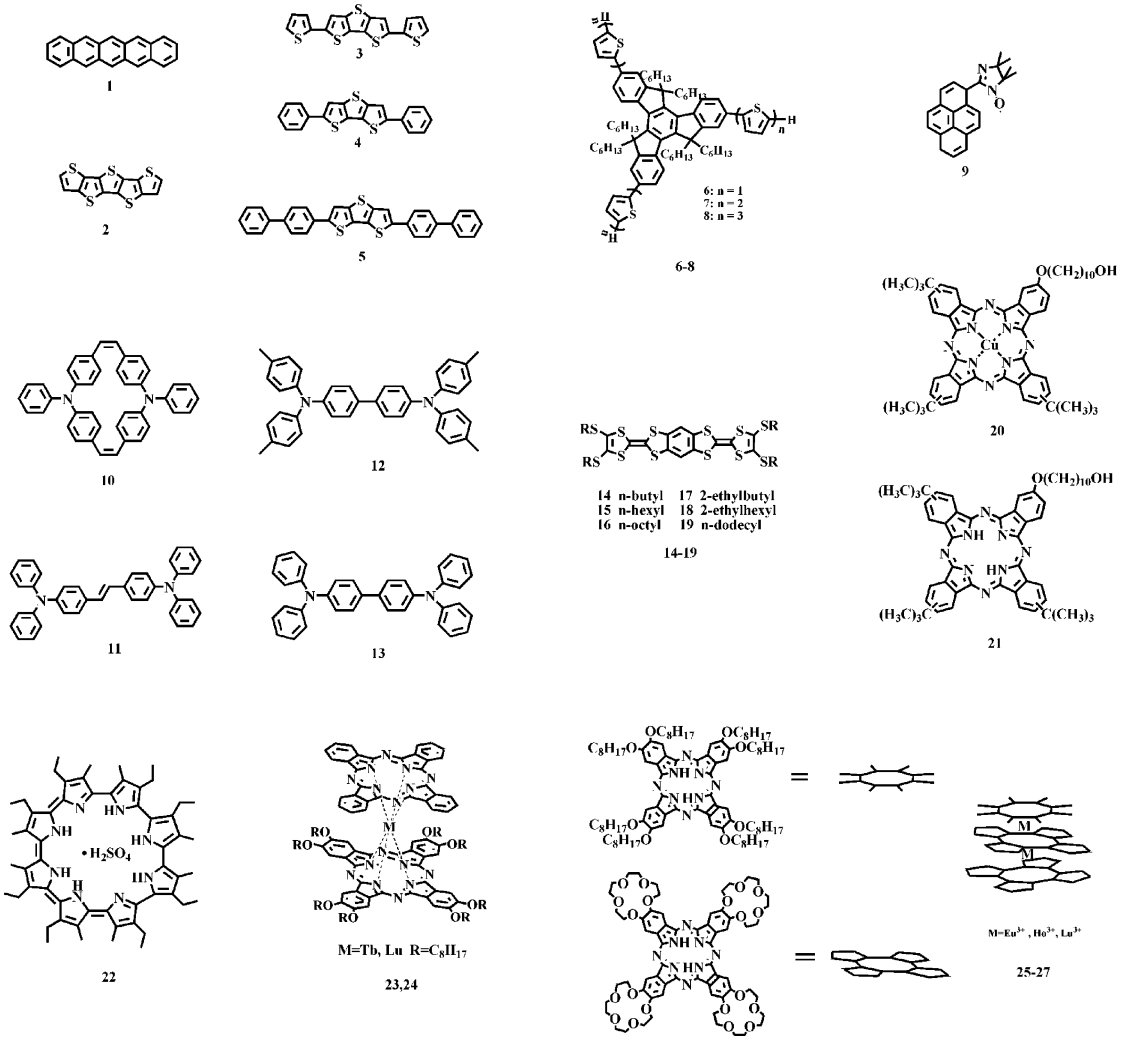

Figure 3. Chemical structures of some organic semiconductors discussed in this article.

the organic semiconductor partly determines its environmental stability. The larger band gap (up to 3.29 eV) of PTA as compared with pentacene indicates that the PTA is not sensitive to visible light. The film condition influences the device performance dramatically. It is generally accepted that devices with larger grains exhibit higher field-effect properties as compared with the devices with the smaller grains or the amorphous film. The grain boundaries in polycrystalline film could trap carriers and prevent effective transport. The active film with larger grains leads to fewer boundaries in the conductive channel and higher device performance. With a large π-conjugated and planar molecular structure, a highly ordered PTA polycrystalline film was formed on the SiO_2 surfaces, depending on the substrate temperature. When the substrate temperature was maintained at 353 K, the crystal grain size was $\sim 0.8 \times 2\ \mu m^2$. The temperature-dependent film characteristics and device performances will be discussed later. Under these circumstances, we obtained a high mobility of 0.045 $cm^2\ V^{-1}\ s^{-1}$ on the bare SiO_2.

As discussed above, oligothiophenes can easily twist from planarity and disrupt the conjugation. An effective approach to resolving the problem is to combine the stability of the thiophene ring with the planarity of linear acenes to produce fused-ring thienoacenes. Dithieno[3,2-*b*:2′,3′-*d*]thiophene (DTT) is an important building block in the synthesis of fused thiophenes.[42] Its derivatives have been extensively used as organic semiconductors in OFETs.[43] A series of new organic semiconductors was designed and synthesized using 2,6-dibromo DTT as the core (see Figure 3, compounds **3**−**5**).[44] For these materials, the optical band gap was estimated be 3.0 eV, which indicates good environmental stability in air. Their stability can be verified by device fabrication and measurement. For OFETs based on compounds **4** and **5**, the device performance (mobility and on/off ratio) was maintained for several weeks without obvious decrease. These results clearly demonstrated that the OFETs based on compounds **4** and **5** have excellent environmental stability. For the organic optoelectronic devices (light-emitting diodes, thin film transistors), carrier injection from the electrodes into the organic layer is of great importance. The energy barrier between the highest occupied molecular orbital (HOMO) (or the lowest occupied molecular orbital (LUMO)) of organic semiconductors and the work function of source−drain electrodes determines the hole (or electron) injection. As an example, for p-type FETs with Au S−D electrodes, efficient hole injection is obtained when the HOMO energy level of organic semiconductors matches well with the work function of a Au electrode. The HOMO energy level of compound **3** was estimated to be −5.18 eV. This value matches well with the work function of gold (Au: 5.1 eV) and can ensure efficient hole injection. Moreover, these semiconductors possess good polycrystalline film-forming properties, and the molecules are oriented in an orderly manner with a $\pi-\pi$ stacking direction parallel to the substrate. The packing model facilitates charge carrier transport. These properties ensured OFETs based on these organic

semiconductors exhibit high device performance and excellent stability. OFET based on compound **4** shows a field-effect mobility of 0.42 $cm^2\ V^{-1}\ s^{-1}$ and an on/off ratio of 5×10^6 on the OTS-modified SiO_2 substrate. For compound **5**, a hole mobility of 0.6 $cm^2\ V^{-1}\ s^{-1}$ was achieved by using polyvinyl alcohol (PVA) as the dielectric layer.[45]

Polymers are attractive for OFET applications since polymer-based devices can be fabricated by various solution techniques, such as spin-coating, drop-casting, printing, etc. Solution fabrication dramatically decreases environmental requirements, simplifies fabrication process, and reduces the device fabrication costs. Theoretically speaking, a solution process can also be achieved for small-molecule semiconductors; however, the strong intermolecular interaction leads to insolubility in common solvents for many excellent organic semiconductors. Polymerization and side-chain substitution are the most effective approaches to improve their solubility in solvents. Another method is the synthesis of star-shaped organic semiconductors.[46] Oligothiophene-functionalized truxene derivatives are a series of star-shaped materials with good solubility.[47] We demonstrate that OFETs based on this solution process, star-shaped, oligothiophene-functionalized truxene derivatives could exhibit satisfactory device performance.[48] As demonstrated by X-ray diffraction data (XRD) measurements, a transition from polycrystalline to an amorphous state occurred with a stepwise increase in the thiophene ring at every branch. The mobility depends greatly on the morphology in the solid state and decreases as the thiophene ring increases. The device performance shares the same trend as compared with the transition. The most excellent mobility of 1.03×10^{-3} $cm^2\ V^{-1}\ s^{-1}$ was obtained for compound **6** in the polycrystalline state. This value is very high for star-shaped organic semiconductors, but it is much lower than those of linear thiophene derivatives. This mainly results from weak intermolecular interactions and disordered molecular packing.

2.2. Macrocycle Derivatives. Triarylamine-based organic semiconductors have been widely investigated for optoelectronic applications.[49,50] As a matter of fact, these materials possess many attributes that meet the requirements for OFET applications. Unfortunately, these materials usually exhibit low field-effect mobilities due to their amorphous film states.[51−54] Triarylamine-based polymers show a similar phenomenon. Amorphous polytriarylamines (PTAA) is a widely studied polymer.[55,56] For PTAA-based OFETs, a maximum mobility close to 0.01 $cm^2\ V^{-1}\ s^{-1}$ was obtained. Although the performance is rather high among amorphous semiconductors, it is much lower as compared with other polymers, such as regioregular poly(3-hexylthiophene). Amorphous film is a crucial reason. A cyclic structure (compound **10**) could solve the problem appropriately.[57] With a closed ring and steric crowded structure, the rotation of the phenyl groups can be restricted. Therefore, planar molecular structure and orderly molecular packing can be achieved. As can be seen from single-crystal characterization, the molecules with a macrocyclic structure were packed into columns along the *b*-axis direction and stacked in a "layer-by-layer" pattern in both the *a*- and *c*-axis directions. Such column and layer-by-layer packing manner could favor hole transport. Table 1 shows the detailed device performance of the cyclic triphenylamine dimer 10 and the linear triphenylamine derivatives. Both the mobility and the on/off ratio of the cyclic triphenylamine 10 are an order of magnitude larger than those of the linear triphenylamine derivatives (see Table 1). Compared with linear triphenylamine derivatives, an orderly polycrystalline film of cyclic triphenylamine dimer can be easily obtained. Grains longer than 2 μm were grown on the OTS-modified SiO_2 surfaces (see Figure 4). The property of good polycrystalline film formation should be responsible for the efficient carrier transport. Using Marcus electron transfer theory and an incoherent Brownian motion model, the hole mobilities of compounds **10** and **11** were estimated to be 2.1×10^{-2} and 1.9×10^{-3} $cm^2\ V^{-1}\ s^{-1}$, respectively. The values match well with the experimental results. All these factors combine to result in the high field-effect characteristics of cyclic triphenylamine-based devices, which represent a promising new choice for the design of organic semiconductors.

TABLE 1: Detailed Device Performance of the Triphenylamine Derivatives

compound	mobility ($cm^2\ V^{-1}\ s^{-1}$)	on/off ratio
10	$\sim 0.5-1.5 \times 10^{-2}$	$\sim 10^6-10^7$
11	$\sim 0.9-2 \times 10^{-4}$	10^4
12	$\sim 1-3 \times 10^{-4}$	10^4
13	$\sim 1-2 \times 10^{-5}$	10^3

Cyclo[8]pyrrole (compound **22**) is an extended porphyrin-like molecule possessing 30 π-electrons.[58] The cyclo[8]pyrrole molecule shows a nearly coplanar conformation, whereas the large expanded porphyrins containing eight or more pyrrole rings often adopt a twisted conformation. Meanwhile, the fully conjugated 30-π- electron system of the cyclo[8]pyrrole molecule has good electron donating ability and favors intermolecular $\pi-\pi$ overlapping. Using the Langmuir−Blodget (LB) film technique, highly ordered cyclo[8]pyrrole films were fabricated. The cyclo[8]pyrrole-based FETs exhibited a high hole mobility of 0.68 $cm^2\ V^{-1}\ s^{-1}$ and a high on/off ratio of 8×10^4.[58] Phthalocyanines (Pc) is a planar and aromatic macrocycle, which consists of four isoindole units presenting 18 π-electrons. A remarkable feature is their versatility. Many different metal elements can replace the hydrogen atoms of the central cavity. One or even two metal atoms may be included in the central cavity of Pc, depending on the size and the oxidation state of the metal atoms. Usually, Pc's are thermally and chemically stable, exhibiting low solubility in common organic solvents. This result is attributed to the strong intermolecular interactions in the solid state of Pc. The strong $\pi-\pi$ interactions could contribute to carrier transport. The field-effect properties of phthalocyanine derivatives such as CuPc,[59] FePc,[60] and F_{16}CuPc[61] have been reported. For devices based on phthalocyanine derivatives, the organic layers were deposited by vacuum sublimation. As discussed above, a solution fabrication technique may dramatically reduce the fabrication cost. Substituents have been introduced into the Pc molecules to increase solution processability. 2,9,16-Tri(*tert*-butyl)-23-(10-hydroxydecyloxy) phthalocyanine (compound **21**) and 2,9,16-tri(*tert*butyl)-23-(10-hydroxydecyloxy) copper phthalocyanine (compound **20**) exhibit good solubility in the common organic solvents, such as chloroform, acetonitrile, and toluene.[62] Therefore, they can be fabricated as the active layer of OFETs by using the LB technique. Although these compounds exhibit a similar energy band gap and HOMO energy level, the device performance suffers from great difference. It results from the fact that the close face-to-face stacking of the compound **20** molecules makes it easy for carrier transport. The ordered molecular assembly of heteroleptic bis(phthalocyaninato) rare earth complexes M(Pc)[Pc-$(OC_8H_{17})_8$] (M = Tb, Lu; H_2Pc = phthalocyanine; $H_2Pc(OC_8H_{17})_8$ = 2,3,9,10,16,17,23,24-octakis-(octyloxy)-phthalocyanine (compounds **23** and **24**) resulted in the mobilities varying from 6.4×10^{-4} to 1.7×10^{-3} $cm^2\ V^{-1}\ s^{-1}$.[63] Tris(phthalocyaninato) rare earth tripledecker complexes (compounds **25**−**27**) possess high mobilities of 0.2−0.6 cm^2

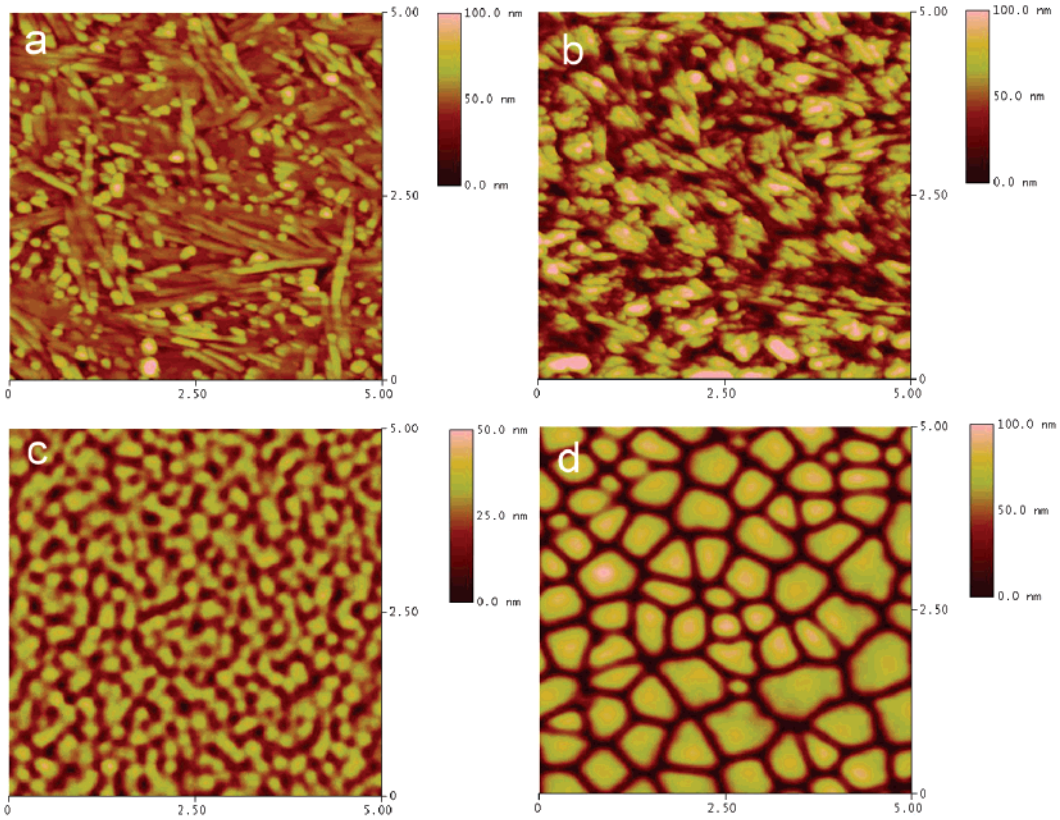

Figure 4. AFM images of the compounds (a) **11**, (b) **10**, (c) **12**, and (d) **13** deposited on the OTS-treated SiO_2 substrates at 285 K. Reprinted from ref 57.

V^{-1} s^{-1}.[64] Although the high performance of these devices is not fully understood, strong intermolecular $\pi-\pi$ stacking, and intermolecular *J* aggregation can contribute to the unexpectedly positive results.

2.3. Organic Radicals. Organic radicals are usually paramagnetic molecules. Some organic radicals possess many advantages, such as a planar molecule structure and a good polycrystalline film-forming property. 1-Imino nitroxide pyrene (compound **9**) is a paramagnetic molecule with an unpaired electron.[65,66] The OFETs using 1-imino nitroxide pyrene as the active layer exhibit the high device performance with a mobility of 0.1 cm^2 V^{-1} s^{-1}, on/off ratio of 5×10^4, threshold voltage of −0.6 V, and subthreshold slope of 540 mV $decade^{-1}$.[66] Two interesting phenomena were observed for 1-imino nitroxide pyrene-based OFETs. First, the devices can be operated with a very low operation voltage. This can be ascribed to the low density of charge traps resulting from the hydrogen bond interactions between the −N−O· of 1-imino nitroxide pyrene and the −OH groups on the SiO_2 surfaces. Furthermore, no obvious reflection peak was obtained by XRD measurements. This result indicated that the organic film was in a disordered orientation. Considering the outstanding field-effect properties of these devices, it can be deduced that the molecules of the first layer were arranged regularly due to the hydrogen bond interactions between the −N−O· of the molecules and the −OH groups on the SiO_2 surface. Then, the ordered arrangement of the first few layers facilitates the carrier transport and leads to a high device performance. As for OFETs, few molecular layers could form a conductive channel.[67] However, a much thicker semiconductor layer is deposited for a typical OFET, because few nanometer thick films cannot give a continuous conductive channel. When a strong interaction between the semiconductor and the dielectric layer existed, continuous channel could be obtained in a very thin film. On the other hand, the interaction could ensure low trap density. As a demonstration, Guo et al. fabricated a monolayer transistor that exhibits high device performance.[68] One of the critical characteristics of this device is the excellent dielectric/organic semiconductor monolayer interface. Therefore, the interaction between the semiconductor and the dielectric layer deserves attention to improve device performance.

2.4. Tetrathiafulvalene. Tetrathiafulvalene (TTF) derivatives have been widely studied as organic conductors and superconductors since the discovery of the first organic metal tetrathiafulvalene-7,7′,8,8′-tetracyanoquinodimethane (TTF-TCNQ) over 30 years ago.[69] These derivatives exhibited strong $\pi-\pi$ stacking together with S···S-interaction-governed intermolecular interactions. On the other hand, the TTF derivatives are generally soluble in various solvents, can be easily chemically modified, and are good electron donors. Tanaka and co-workers first reported the TTF-based OFETs.[70] Recently, various TTF derivatives have been designed as organic semiconductors. By using the vacuum deposition technique, biphenyl-substituted TTF (DBP-TTF)-based FETs exhibited a mobility of 0.11 cm^2 V^{-1} s^{-1}.[71] To enhance the air stability and decrease the electron-donating ability, fused aromatic rings were introduced into the TTF molecules. The TTF derivatives with aromatic fused benzene rings and nitrogen heterocycles were reported. These compounds exhibit high field-effect mobilities up to 0.4 cm^2 V^{-1} s^{-1} and good stabilities.[72] A mobility as high as 1.4 cm^2 V^{-1} s^{-1} was obtained from DT−TTF single-crystal devices using solution processing.[73] Recently, we have developed a one-step synthesis of benzene-fused bis-TTFs without central substituents (compounds **14**−**19**), which could form efficient intermolecular $\pi-\pi$ stacks.[74,75] The device based on compound **15** afforded the highest mobility, 0.02 cm^2 V^{-1} s^{-1}. The

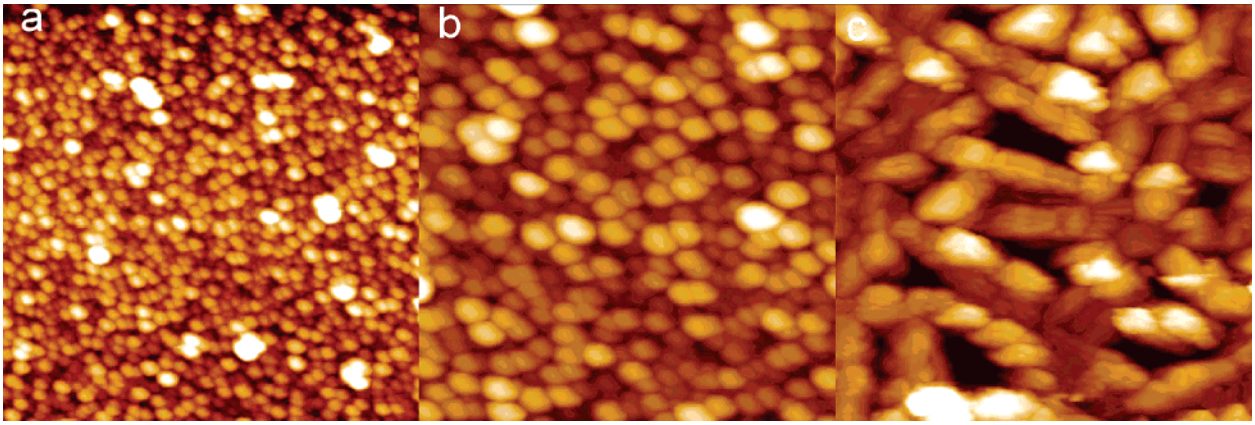

Figure 5. A 5 × 5 μm^2 AFM image of the PTA film on the SiO_2/Si substitute fabricated at (a) room temperature, (b) 60 °C, and (c) 80 °C. All of the AFM images were taken in contact mode. Reprinted from ref 36.

performance is quite high among solution-processed thin film FET devices based on small organic molecules. However, similar to the devices based on many other TTF derivatives, these devices suffered from a low on/off ratio due to the existence of rich carriers in the active layer. This problem could be resolved by the introduction of electron-withdrawing groups. It has been proved that the introducing halogen groups lead to obvious improvement of both the carrier mobility and the on/off ratio for the TTF derivatives based FETs.[13]

3. Device Fabrication and Physical Properties

Although the organic semiconductors play a dominant role in determining the properties of OFETs, the device performance is also influenced by various other factors, such as organic semiconductor deposition conditions, dielectric layer properties, and organic electrode/organic layer contact. Recently, improving device performance by controlling device fabrication conditions has received special interest. In this section, we will discuss a few factors that influence device performance, including device fabrication techniques, dielectric−organic layer contact, and source−drain electrode−organic contact.

3.1. Device Fabrication Techniques. The condition of the organic thin film greatly influences carrier transport properties. Devices fabricated with different techniques can exhibit varied field-effect properties. Therefore, fabrication techniques for making the active layers have received much attention. Until now, vacuum evaporation and solution process have been the most widely applied methods to fabricate organic active films.

Vacuum evaporation is an effective way to fabricate thin films of the small organic molecules. Organic semiconductor films are deposited by sublimation in a chamber under high vacuum. To achieve a highly ordered film, the deposition conditions have to be strictly controlled. Substrate temperature and evaporation rate are the most important factors influencing the film conditions. Larger grains can usually be obtained by increasing the substrate temperature. An ordered film with fewer boundaries in the active channel could improve the device performance. Figure 5 shows the AFM image of the PTA film on the bare SiO_2 surface fabricated at different substrate temperatures. Densely packed grains with an average diameter of about 300−600 nm were obtained at a substrate temperature of 25 °C. The size of the crystal grains increased with the substrate temperature. When the substrate temperature was 80 °C, the crystal grains were relatively large and elongated in shape, with an average grain size of ∼0.8 × 2 μm^2. The large grains resulted in many fewer boundaries and increased the mobility from 0.0043 to 0.045 $cm^2\ V^{-1}\ s^{-1}$. However, the high substrate temperature does not necessarily result in high device performance, despite large polycrystalline grains. When large grains go along with large grain boundaries, the conductive channel is discontinuous. Therefore, the device performance could decrease dramatically. For example, the cyclic triphenylamine dimmer exhibited the highest performance at a substrate temperature of 20 °C. When the temperature was maintained at 60 °C, the extracted mobility decreased by 2 orders of magnitude due to the discontinuity of the active channel.[57]

The evaporation rate is another factor influencing the film conditions. A lower evaporation rate usually leads to larger grains, whereas a higher rate results in smaller ones. Figure 6 shows the AFM image of compound **10** under different evaporation rates. We obtained a large grain size up to 1 × 1 μm^2 when the evaporation rate was maintained at 0.4 Å/s. However, no obvious field effect was observed due to the discontinuity of the conductive channel caused by large boundaries. This problem can be resolved by increasing the deposition rate to 2 Å/s, which gives rise to a continuous film with smaller grains. A field effect mobility of $10^{-4}\ cm^2\ V^{-1}\ s^{-1}$ can be obtained. Therefore, both the larger grains and the interconnectivity in the channels have a dramatic influence on the device performance. A similar phenomenon was also observed for the pentacene devices. Both the large grain size and excellent interconnectivity can be achieved by controlling the deposition rate of pentacene. Hwa Sung Lee et al. realized high-performance pentacene devices fabricated by controlling the deposition rate (first layer 10 nm, 0.1 Å s^{-1}; second layer 40 nm, 4.0 Å s^{-1}).[76] A slow evaporation rate for first-layer pentacene ensured a large grain size; the following layer deposited at high speed could fill the gaps between large grains. The remarkable performance resulted from the interconnectivity between pentacene grains. Tetracene-based devices also exhibited a similar trend. When the film of tetracene was deposited on a SiO_2 surface at a higher speed (>3 Å s^{-1}), the OFETs based on tetracene exhibited the best device performance, despite small grains and high boundary density.[77] Thus, it can be concluded that uniform substrate coverage dominates over the density of grain boundaries in determining tetracene device performance on the SiO_2 surface.

Fabrication of the organic active layer using solution methods has attracted wide interest due to potential applications for ultralow cost organic devices. Spin-coating, drop-casting, and printing techniques are the most frequently used solution approaches. As far as organic semiconductors are concerned,

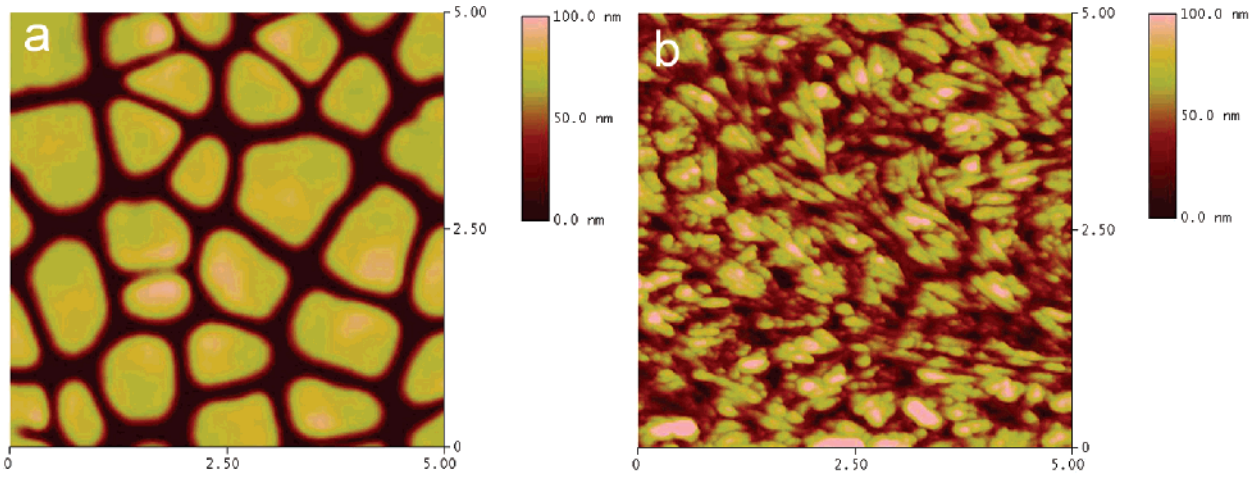

Figure 6. AFM images of the BDPAS film deposited on the OTS-treated SiO_2 surface with a deposition rate of (a) 0.4 and (b) 2 Å/s.

both the thin film of polymer and small molecules can be fabricated using solution methods. Polymers are the most widely studied solution processing materials. To achieve efficient charge transport, polymers composed of microcrystallines are preferable. Regioregular poly(3-hexylthiophene) (P3HT) is a well-studied polymer with a high hole mobility of 0.1−0.3 $cm^2\ V^{-1}\ s^{-1}$.[78,79] The P3HT films adopt a highly microcrystalline and anisotropic lamellar microstructure comprising two-dimensional conjugated layers with strong interchain interactions separated by layers of soluble and insulating side chains. This microstructure contributes to effective in-plane charge transport.[80] However, it is difficult to obtain ordered molecule packing for the solution processed semiconductor because the microcrystalline structure relies on self-organization of the solution during the fabrication process. Annealing of the fabricated films provides an excellent approach to achieve an ordered film from the solution process.[17] The thermal annealing may significantly decrease the effect of the residual solvent on the carrier transport. After the thermal annealing, a high-order film similar to the vacuum deposited form could be formed, resulting in few boundaries and efficient carrier transport. Small molecule semiconductors can also be processed with solution methods. The pentacene precursors have been reported.[81,82] After formation of the precursors' film using the solution approach, thermal annealing and UV irradiation were utilized to return to the pentacene film. The film retained high carrier transport ability. Another way to achieve solution-processing of small molecules is side-chain substitution. Katz reported side-chain-substituted small molecules,[83] dihexylanthradithiophene, that can be solution-deposited with the mobilities of 0.01−0.02 $cm^2\ V^{-1}\ s^{-1}$. We demonstrated that a series of star-shaped oligothiophene-functionalized truxene derivatives can be processed by a solution process.[48] As mentioned above, a transition from polycrystalline to an amorphous state was observed with an increase in the thiophene ring at every branch. This transition leads to a decrease in the device performance. Triethylsilylethynyl anthradithiophene is another p-type solution-processing organic semiconductor.[84] After thermal annealing, large, continuous, and highly crystalline grains spanning from several hundred micrometers to several millimeters were obtained.[85] Hexabenzocoronene (HBC) derivatives exhibit outstanding solubility. Under a high magnetic field during the solvent evaporation process, molecules of hexa(4-dodecylphenyl)hexa-*peri*-hexabenzocoronene (HBC-PhC_{12}) were orderly aligned, resulting in large-area monodomains and high device performance.[86] As discussed above, ordered molecule packing favors device high performance.

3.2. Dielectric Layer-Organic Semiconductor Contact. The dielectric layer is an important element of OFETs. Its chemical composition, surface morphology (roughness), and dielectric properties have dramatic influence on the condition of the organic thin films and the device performance. Silicon dioxide (SiO_2) is widely used as the dielectric layer because of its excellent insulating property and stability as well as its low surface roughness. However, small grains are usually obtained when organic semiconductors are deposited on the bare SiO_2 surface. It limits the improvement of the device performance. Modification of the SiO_2 surface using a self-assembly monolayer such as octadecyltrichorosilane (OTS) or hexamethyldisilazane (HMDS) has been widely explored to enhance the device performance. The surface modification usually leads to an increased contact angle, enlarged semiconductor grains, a reduction of the trap density, and an improvement in the device performance. Aside from the self-assembly monolayer modification method, the active film morphology can also be improved by the introduction of a buffer layer between the organic semiconductor and the dielectric layer. C_{60} thin films grown on the SiO_2 dielectric layer exhibit poor orientation, resulting in poor performance of the device. A smooth pentacene monolayer used as a buffer enhanced the molecular wettability of the substrate and, thus, improved the crystallinity of C_{60}.[24] The crystallinity enhancement increased the field-effect mobilities of the C_{60} transistors to 2.0−4.9 $cm^2\ V^{-1}\ s^{-1}$. The device performance undergoes a 4- to 5-fold improvement over that of the C_{60} films grown without the pentacene buffer layer. One obstacle for SiO_2-based devices to achieve widespread application is the higher operation voltage of these devices, which is typically >20−50 V. The high operating voltage will result in excessive power consumption. This problem could be solved by increasing the dielectric capacitance by either using a gate insulator with higher dielectric constant or by reducing the thickness of the insulator. Reducing the thickness usually gives rise to a larger leak current. Therefore, a higher dielectric constant layer should be explored. Until now, many high-k oxides, such as barium zirconate titanate (BZT, k (bulk) = 17.3),[87] barium strontium titanate (BST, k (bulk) = 16),[87] Si_3N_4 (k (bulk) = 6.2),[87] and Ta_2O_5,[88] have been used as the dielectric layers. When a dielectric layer with a higher dielectric capacitance is used, a much lower operating voltage can induce a high carrier density at the dielectric layer−organic active layer

interface. As a result, operating voltages below 5 V have been achieved.

A solution processing dielectric layer is attractive for use in flexible devices. The polymer dielectric layer can be processed by solution approaches, such as spin-coating, casting, or printing, at room temperature and under ambient conditions. A number of polymer dielectric materials have been developed.[89−92] Using the polymer dielectric layer usually leads to higher performance, lower operating voltage, or both. Varied organic film morphology can be formed on different polymer dielectric layers. The grain sizes of the pentacene deposited on the HMDS-modified SiO_2/Si or polystyrene (PS) substrates are much larger than those observed on the PVA substrates.[93] Recently, using 5,5′-bis-biphenyl-dithieno[3,2-*b*:2′,3′-*d*]thiophene (BPDTT) as the organic active layer and PVA as the dielectric layer, we achieved a high field-effect mobility of 0.6 $cm^2\ V^{-1}\ s^{-1}$ and an operation voltage lower than 1 V.[45] The higher device performance is mainly attributed to the close herringbone packing of the BPDTT molecules and the high homogeneity between the PVA and BPDTT molecules.[45] The trap density at the insulator interface plays an important role in determining the field-effect properties of the n-type devices because electrons can be easily trapped.[93] Pentacene is a widely used p-type organic semiconductor. An n-type pentacene transistor was realized by Ca interface doping. When Ca was doped into the interface, a large number of electron traps were filled, allowing for an accumulation of mobile electrons at the insulator surface. An electron field-effect mobility of 0.19 $cm^2\ V^{-1}\ s^{-1}$ was achieved.[94] Lay-Lay Chua et al. reported that the use of an appropriate hydroxyl-free gate dielectric divinyltetramethylsiloxane-bis(benzocyclobutene) derivative (BCB) could yield an *n*-channel FET conduction in most conjugated polymers.[95] Interestingly, the traps at the insulator interface were used in nonvolatile memory applications. Baeg et al. reported the memory devices based on OFETs.[96] By introducing a thin layer of a chargeable polymer as the "electret" between the insulating material (silicon dioxide) and the organic semiconductor, the device realized data storage. Therefore, the traps at the insulator interface could be exploited for new applications.

3.3. Source-Drain Electrode-Organic Semiconductor Contact. Carrier injection from the S−D electrode into the organic layer is very important for OFET devices. The carrier injection barrier mainly depends on the barrier between the work function of the metal electrode and the HOMO or LUMO energy level of the organic semiconductors. Selecting the proper S−D electrodes is an effective approach to reduce the carrier injection barrier. Gold is widely used as S−D electrodes to fabricate the p-type OFETs. However, the work function of Au is energetically incompatible with the LUMO energy level of the organic semiconductors. To increase electron injection, low work function electrodes such as Ca and Ag are usually used as the S−D electrodes. Using these metal electrodes, OFETs based on some organic semiconductors recognized as p-type, such as CuPc,[97] pentacene,[94] and rubrene[98] (single crystal), could exhibit ambipolar or n-type operation characteristics or both. The design of new organic semiconductors with proper LUMO energy levels is also an efficient method to improve electron injection. Thomas D. Anthopoulos et al. have reported ambipolar OFETs and an inverter using bis(4-dimethylaminodithiobenzyl)nickel (nickel dithiolene) as the organic active layer and Au as the S−D electrodes.[99] Despite the high work function of the Au electrode, the matched LUMO energy level ensures a low electron injection barrier.

The contact between the organic semiconductor and the S−D electrodes has a significant influence on the field-effect properties. Devices with top-contact geometry usually exhibit good electrode−semiconductor contact and efficient carrier injection. However, it has recently been demonstrated that large carrier injection barriers still exist in some top-contact devices. For this configuration, the metal electrodes are deposited onto the organic layers, which can result in a complicated reaction at the metal/organic interfaces. As an example, pentacene-based devices suffer from bad electrode/semiconductor contact. When Au and Ag were deposited onto the pentacene film, a large hole injection barrier up to 1 eV appeared due to metal penetration into the organic layer and formation of metal clusters.[100,101] The phenomenon has been further demonstrated by studying the effect of the metal penetration on the properties of the pentacene-based devices. By controlling the Au deposition rate, the degree of Au atom penetration can be controlled, resulting in different device performance. A slow gold evaporation rate gave a poor carrier injection because the gold atoms penetrated into the pentacene layer. A high evaporation rate resulted in higher performance due to the formation of a sharp electrode/pentacene contact and little Au penetration.[101] The introduction of a buffer layer between the electrode and the active layer can also improve the device performance. When 7,7,8,8-tetracyanoquinodimethane (TCNQ) was inserted between the metal electrode and the organic layer, the device performance was obviously improved.[102] Another interesting report is the application of Al/MoO_3 as the S−D electrode. The pentacene device with the Al/MoO_3 electrodes exhibited device performance higher than that of the gold-based one.[103] The introduced layer reduced the injection barrier and impeded electrode metal penetration.

The top contact geometry exhibits a significant obstacle to manufacturability application, that is, incompatibility with the photolithographic process. Shadow masking is generally used to fabricate the top-contact devices. Therefore, the channel length is usually larger than 20 μm, which limits their real applications. The bottom contact configuration is a feasible geometry in practical application. Unfortunately, the devices with bottom contact suffer from lower performance due to bad metal/organic contact. The bad contact can be properly resolved by self-assembly of a single-molecule layer containing −SH.[104,105] The modified device showed a much higher linear region mobility. Using a conducting polymer[106] and carbon nanotubes[107] as the S−D electrodes could also provide good electrode/semiconductor contacts. Recently, carboxylic acid-modified silver nanoparticles have been successfully used as S−D electrodes to fabricate high-mobility OFETs.[18] The result indicated that chemical modification of the low-cost electrodes is an efficient way to fabricate low-cost, high-performance OFETs. As far as p-type OFETs are concerned, to use low-cost metals such as Ag or Cu as the S−D electrodes, both the enhancement of the work function and improvement of the electrode/semiconductor contact are required. More recently, we fabricated high-performance, low-cost pentacene-based devices with chemically modified Cu or Ag electrodes.[19] The Ag or Cu S−D electrodes were modified with a very simple method by dipping TCNQ solution onto the patterned electrodes. TCNQ can easily react with Cu or Ag to form the charge-transfer compound Cu-TCNQ or Ag-TCNQ. The formation of the charge-transfer compounds obviously enhanced the work function of the S−D electrodes, decreasing the hole injection barrier. The electrode modification also improved the physical contact between the electrode and the semiconductor. The reduced injection barrier and improved contact dramatically reduced contact resistance. In a typical OFET device, when the space charge-limited current (SCLC) effects are neglected, the total

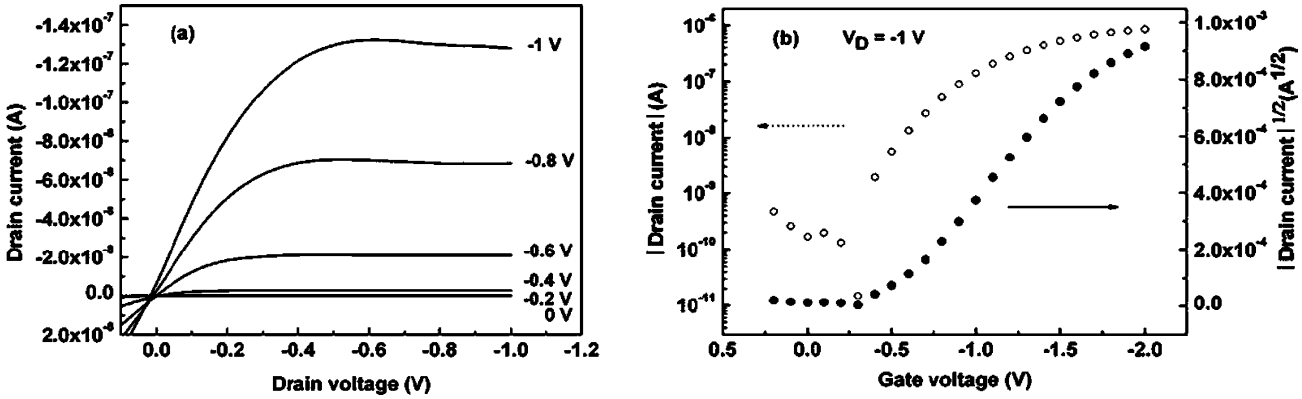

Figure 7. Electrical characterization for OTFTs based on BPDTT. (a) Drain current vs drain−source voltage characteristics. (b) Transfer curve in the saturated regime at drain−source voltage of −1 V and square root of the absolute value of the current vs the gate voltage. Reprinted from ref 45 with permission. Copyright 2006 American Institute of Physics.

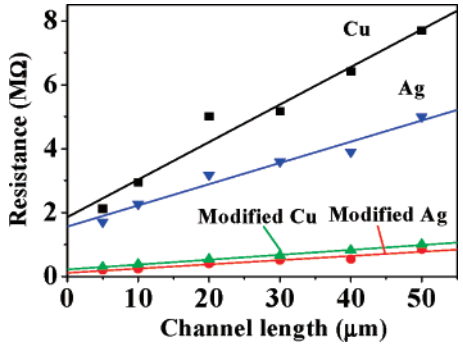

Figure 8. Analysis of contact resistances for pentacene-based devices with various electrodes. Reprinted from ref 19.

on-state resistance in the linear operation regime ($V_{DS} \ll V_{GS}$), R, consists of channel resistance and contact resistance and can be expressed as follows:[108,109]

$$R = R_{ch}L + 2R_{S/D}$$

where R_{ch} is the channel resistance per unit channel length, and $R_{S/D}$ is the contact resistance between the electrode and the organic semiconductor. When R is plotted as a function of L, the contact resistance between the S−D electrode and pentacene can be obtained. The contact resistance was dramatically reduced after the electrode modification (see Figure 8). This can be further testified by the output characteristics for the device with a channel length of less than 10 μm, where the contacts usually become problematic in organic transistors. Figure 9 shows the output characteristics of the devices (channel length of 5 μm) with the Cu and modified Cu electrodes. The devices with a bare Cu electrode suffer from large contact resistance and exhibited S-shaped characteristics in the linear regimes. In comparison, the OFETs with modified electrodes exhibited ideal ohmic contact characteristics: a linear $I_{DS}-V_{DS}$ relationship in the linear regimes. The modification approach has been applied to many OFETs based on different organic semiconductors. This method constitutes a general way to fabricate OFETs with both high performance and low cost.

3.4. Single-Crystal FETs. The chemical purity affects the device performance to a very large extent. A high-purity organic layer usually leads to an excellent performance. Meanwhile, the boundaries in the active film limit charge carrier transport in the channel, since the carrier may be trapped. However, OFETs based on single crystals can provide a high-purity organic active channel, ordered molecular packing with minimum trap, and excellent carrier transport properties. Nowadays, pentacene-based single-crystal FET with a maximum mobility of 40 cm^2 V^{-1} s^{-1} has been obtained.[110] Rubrene single-crystal FETs have exhibited an high mobility of 15 cm^2 V^{-1} s^{-1}.[111] It has been demonstrated that single-crystal devices based on several semiconductors such as CuPc,[112] rubrene,[113] and TCNQ,[113] exhibit higher device performance, as compared with that of their thin-film based FETs. Moreover, the devices based on single crystals provide an ideal active layer to perform organic semiconductor conduction mechanism research.

Recently, improving the fabrication techniques of single-crystal OFETs has become an important research area. Top-gate geometry is a frequently reported configuration for single-crystal FETs. In this geometry, the dielectric layer and gate electrode are fabricated on the single crystal. Many methods, including the flip-crystal technique,[114] elastomeric stamp platforms,[115] and freestanding devices,[112] have been used to fabricate top-gate electrodes. However, most of the reported single-crystal devices contained a relatively thick (5−500 μm) single crystal, leading to the following problems. First, the large-size single crystals are difficult to grow. Furthermore, the large scale creates a processing challenge due to its fragility. These drawbacks limit their wide application in sensors or plastic transistors for flexible electronics.[116] Decreasing the size of the single crystal can overcome these problems. Bao et al. reported a high-performance, thin rubrene single-crystal-based device on a flexible substrate.[116] The organic single-crystal size was decreased to form single-crystalline nanoribbons or microribbons. Submicro- and nanometer device fabrication and characterization not only provide a deep understanding conducting mechanism but also give an effective way toward nanoelectronics. Different devices based on single crystals of micro- or nanometer scale, such as CuPc and F_{16}CuPc, have been reported.[117,118] All the devices exhibited high performance.

More recently, we fabricated OFETs based on perylo[1,12-*b*,*c*,*d*]thiophene (PET) micrometer single-crystal wires.[119] By using a physical vapor deposition technique, the micrometer single-crystal wire was formed on the OTS-treated SiO_2 substrate. The devices exhibited a mobility (0.8 cm^2 V^{-1} s^{-1}) higher than that of the polycrystalline film based device (0.05 cm^2 V^{-1} s^{-1}). These results again indicated that the boundaries in polycrystalline film have a remarkable influence on the carrier transport, and the single-crystal device fabrication is a novel way to present the natural electric properties of the organic semiconductors. Combined with single crystal analysis, we found that the planar PET molecules were stacked along the *b*-axis with interplanar distances of 3.47 Å, in contrast to the sandwich herringbone packing of the perylene crystals. Interest-

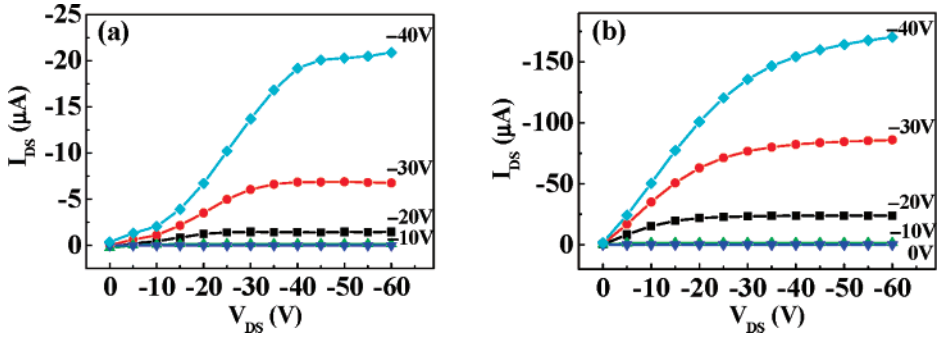

Figure 9. Output characteristics of the devices with channel length of 5 μm and the S−D electrode of (a) Cu and (b) Cu-TCNQ modified Cu electrode. Reprinted from ref 19.

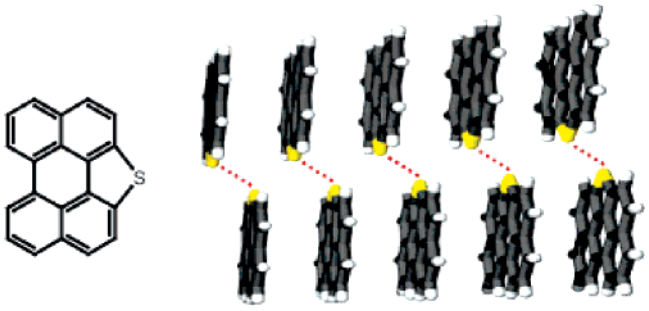

Figure 10. Chemical structure and crystal packing view of PET. Reprinted from ref 119.

ingly, S···S short contacts (3.51 Å) were observed between the neighboring columns related by an inversion center (see Figure 10).[119] Consequently, the double-channel fashion could facilitate the carrier transport and is responsible for the high performance. A similar phenomenon was observed for hexathiapentacene (HTP),[120] which possesses a short S···S interaction in addition to the $\pi-\pi$ stacking. Therefore, the combination of the single-crystal structure and single-crystal device performance can provide a deep understanding of the molecular conduction mechanism. Another interesting research area in the field of single-crystal FETs is the patterning of single crystals. Despite their high extracted device performances, single-crystal FETs were with little expectation in real application within the past few years due to the difficulty in the device fabrication and effective patterning. The single-crystal location and orientation patterning is indispensable for the further development of single-crystal FETs. The vapor deposition method is widely applied to prepare organic single crystals. The substrate surface conditions affect the single-crystal growth dramatically. When single crystals of thiophene/phenylene co-oligomers were epitaxially grown on a single-crystal substrate of potassium chloride (KCl), the needle-shaped crystals were aligned perpendicular to the crystal needle axis.[121,122] Using physical vapor deposition, tetracene single crystals with good crystallographic orientation were also growth on the substrate with thermotropic liquid crystal solvents.[123] More recently, Bao et al. reported an exciting result of effective patterning for organic single crystals.[124] They discovered that many organic semiconductors, such as pentacene, rubrene, and C_{60}, could grow on stamped OTS domains. Therefore, patterning of nucleation location and nucleation density of molecular single crystals can be realized. Despite this important advance, the orientation and alignment of the crystals are still far from satisfactory. When the location and the orientation of organic single crystals can be controlled exactly, the organic single-crystal FETs which possess much higher device performance might replace the thin film OFETs in real applications.

4. Conclusion

Over the past few years, tremendous progress has been achieved in organic semiconductros and their devices, whose mobilities are comparable to those of amorphous silicon FETs. The design of organic semiconductors, a deep understanding of both hole and electron transport in organic semiconductors, exploration of new applications, and fabrication of low-cost flexible OFETs have received significant interest; however, both opportunities and challenges exist in further development of OFETs toward applications. Design of novel materials, optimization of the device structures, and the exploration of applications deserve continued focus in the future.

Molecular design and synthesis are the most important challenges. To meet the further development of OFETs, new organic semiconductors with high carrier mobility, excellent stability, and low cost are still desirable. Carrier transport ability relies greatly on the molecular packing and intermolecular interactions; however, their relationships are not fully understood. Therefore, a deep understanding of the relationship between the molecular structure, packing model, and device performance could be helpful for the molecular design. With respect to stability, both the environmental and operational ones are very important. Organic semiconductors with high environmental stability could withstand the influence induced by environmental conditions such as light irradiation and O_2 doping, etc. The operational stability is related to the operation lifetime of devices in the operational state. When the OFETs are in the operational state, the high carrier density in the active channel can prevent a decrease in the device performance. Both the high environmental and operational stabilities are necessary to enable the applications of OFETs. Solution processing of high performance organic semiconductors is always a subject with great opportunity to achieve low-cost, flexible, organic electronics.

An even more challenging subject is the design of multifunctional organic materials. The multifunctional organic materials may combine two or more kinds of physical properties and exhibit different properties under different circumstances. For example, organic semiconductors with both excellent light emission properties and field-effect characteristics have been applied as the active layer in organic light-emitting field-effect transistors. Therefore, exploration of multifunctional organic semiconductors should provide an effective method to develop integrated devices, reduce fabrication cost, and fabricate multifunctional devices.

Device optimization could promote further advancement of OFETs. All the device components, including the organic active

layer, the dielectric layer, and the electrodes, are indispensable and influence the device performance. Different organic semiconductors require different deposition conditions, dielectric surface states, and electrodes to obtain optimized film morphology, minimized trap density, efficient carrier injection, and in turn, maximum device performance. Consequently, the relationship between the device fabrication process and device performance requires more exact examination. New device design and application explorations are promising research areas. Novel designed devices will bring on a better understanding of the device physics, improvement of performance, and new application areas. Until now, a number of applications have been demonstrated, and the exploration of new applications will undoubtedly accelerate the development of OFETs.

In summary, tremendous progress has been made in the past few years. High performance OFETs have been obtained. However, it will take a long time to realize flexible OFETs with both high performance and low cost, which will give the true benefits of organic electronics.

Acknowledgment. This work is supported by the National Natural Science Foundation of China (90206049, 20472089, 20421101, 60671047, 50673093), the Major State Basic Research Development Program (2006CB806200, 2006CB932100), and the Chinese Academy of Sciences.

References and Notes

(1) Tang, C. W.; Van, Slyke, S. A. *Appl. Phys. Lett*. **1987**, *51*, 913.
(2) Kudo, K.; Yamashina, M.; Moriizumi, T. *Jpn. J. Appl. Phys., Part 1* **1984**, *23*, 130.
(3) Edman, L.; Pauchard, M.; Liu, B.; Bazan, G.; Moses, D.; Heeger, A. J. *Appl. Phys. Lett.* **2003**, *82*, 3961.
(4) Shaheen, S. E.; Brabec, C. J.; Sariciftci, N. S.; Padinger, F.; Fromherz, T.; Hummelen, J. C. *Appl. Phys. Lett.* **2001**, *78*, 841.
(5) He, Y.; Hattori, R.; Kanicki, J. *Jpn. J. Appl. Phys., Part 1* **2001**, *40*, 1199.
(6) Nelson, S. F.; Lin, Y. Y.; Gundlach, D. J.; Jackson, T. N. *Appl. Phys. Lett.* **1998**, *72*, 1854.
(7) Wu, Y. L.; Li, Y. N.; Gardner, S.; Ong, B. S. *J. Am. Chem. Soc*. **2005**, *127*, 614.
(8) Li, Y. N.; Wu, Y. L.; Gardner, S.; Ong, B. S. *Adv. Mater*. **2005**, *17*, 849.
(9) Facchetti, A.; Mushrush, M.; Yoon, M. H.; Hutchison, G. R.; Ratner, M. A.; Marks, T. J. *J. Am. Chem. Soc.* **2004**, *126*, 13859.
(10) Letizia, J. A.; Facchetti, A.; Stern, C. L.; Ratner, M. A.; Marks, T. J. *J. Am. Chem. Soc.* **2005**, *127*, 13476.
(11) Moon, H.; Zeis, R.; Borkent, E. J.; Besnard, C.; Lovinger, A. J.; Siegrist, T.; Kloc, C.; Bao, Z. N. *J. Am. Chem. Soc.* **2004**, *126*, 15322.
(12) Briseno, A. L.; Roberts, M.; Ling, M. M.; Moon, H.; Nemanick, E. J.; Bao, Z. N. *J. Am. Chem. Soc.* **2006**, *128*, 3880.
(13) Naraso; Nishida, J. I.; Kumaki, D.; Tokito, S.; Yamashita, Y. *J. Am. Chem. Soc*. **2006**, *128*, 9598.
(14) Ando, S.; Murakami, R.; Nishida, J. I.; Tada, H.; Inoue, Y.; Tokito, S.; Yamashita, Y. *J. Am. Chem. Soc.* **2005**, *127*, 14996.
(15) Meng, H.; Sun, F. P.; Goldfinger, M. B.; Jaycox, G. D.; Li, Z. G.; Marshall, W. J.; Blackman, G. S. *J. Am. Chem. Soc.* **2005**, *127*, 2406.
(16) McCulloch, I.; Heeney, M.; Bailey, C.; Genevicius, K.; MacDonald, I.; Shkunov, M.; Sparrowe, D.; Tierney, S.; Wagner, R.; Zhang, W.; Chabinyc, M. L.; Kline, R. J.; McGehee, M. D.; Toney, M. F. *Nat. Mater*. **2006**, *5*, 328.
(17) Ong, B. S.; Wu, Y. L.; Liu, P.; Gardner, S. *Adv. Mater*. **2005**, *17*, 1141.
(18) Wu, Y. L.; Li, Y. N.; Ong, B. S. *J. Am. Chem. Soc.* **2006**, *128*, 4202.
(19) Di, C. A.; Yu, G.; Liu, Y. Q.; Xu, X. J.; Wei, D. C.; Song, Y. B.; Sun, Y. M.; Wang, Y.; Zhu, D. B.; Liu, J.; Liu, X. Y.; Wu, D. X. *J. Am. Chem. Soc.* **2006**, *128*, 16418.
(20) Murphy, A. R.; Fréchet, J. M. J. *Chem. Rev.* **2007**, *107*, 1066.
(21) Zaumseil, J.; Sirringhaus, H. *Chem. Rev.* **2007**, *107*, 1296.
(22) Baude, P. F.; Ender, D. A.; Haase, M. A.; Kelley, T. W.; Muyres, D. V.; Theiss, S. D. *Appl. Phys. Lett.* **2003**, *82*, 3964.
(23) Meng, H.; Sun, F. P.; Goldfinger, M. B.; Gao, F.; Londono, D. J.; Marshal, W. J.; Blackman, G. S.; Dobbs, K. D.; Keys, D. E. *J. Am. Chem. Soc.* **2006**, *128*, 9304.
(24) Itaka, K.; Yamashiro, M.; Yamaguchi, J.; Haemori, M.; Yaginuma, S.; Matsumoto, Y.; Kondo, M.; Koinuma, H. *Adv. Mater.* **2006**, *18*, 1713.
(25) Dimitrakopoulos, C. D.; Malenfant, P. R. L. *Adv. Mater.* **2002**, *14*, 99.
(26) Horowitz, G. *Adv. Mater.* **1998**, *10*, 365.
(27) Horowitz, G. *J. Mater. Res.* **2004**, *19*, 1946.
(28) Horowitz, G.; Hajlaoui, R.; Delannoy, P. *J. Phys. III (Paris)* **1995**, *5*, 355.
(29) Sun, Y. M.; Liu, Y. Q.; Zhu, D. B. *J. Mater. Chem.* **2005**, *15*, 53.
(30) Warta, W.; Stehle, R.; Karl, N. *Appl. Phys. A: Mater. Sci. Process.* **1985**, *36*, 163.
(31) Ostroverkhova, O.; Cooke, D. G.; Shcherbyna, S.; Egerton, R. F.; Hegmann, F. A.; Tykwinski, R. R.; Anthony, J. E. *Phys. Rev. B: Condens. Matter Mater. Phys.* **2005**, *71*, 035204.
(32) Podzorov, V.; Menard, E.; Borissov, A.; Kiryukhin, V.; Rogers, J. A.; Gershenson, M. E. *Phys. Rev. Lett.* **2004**, *93*, 086602.
(33) Troisi, A.; Orlandi, G. *Phys. Rev. Lett.* **2006**, *96*, 086601.
(34) Hulea, I. N.; Fratini, S.; Xie, H.; Mulder, C. L.; Iossad, N. N.; Rastelli, G.; Ciuchi, S.; Morpurgo, A. F. *Nat. Mater.* **2006**, *5*, 982.
(35) Ito, K.; Suzuki, T.; Sakamoto, Y.; Kubota, D.; Inoue, Y.; Sato, F.; Tokito, S. *Angew. Chem., Int. Ed.* **2003**, *42*, 1159.
(36) Xiao, K.; Liu, Y. Q.; Qi, T.; Zhang, W.; Wang, F.; Gao, J. H.; Qiu, W. F.; Ma, Y. Q.; Cui, G. L.; Chen, S. Y.; Zhan, X. W.; Yu, G.; Qin, J. G.; Hu, W. P.; Zhu, D. B. *J. Am. Chem. Soc.* **2005**, *127*, 13281.
(37) Yamada, M.; Ikemoto, I.; Kuroda, H. *Bull. Chem. Soc. Jpn.* **1988**, *61*, 1057.
(38) Marseglia, E. A.; Grepioni, F.; Tedesco, E.; Braga, D. *Mol. Cryst. Liq. Cryst.* **2000**, *348*, 137.
(39) Barbarella, G.; Zambianchi, M.; Bongini, A.; Antolini, L. *Adv. Mater.* **1993**, *5*, 834.
(40) Ichikawa, M.; Yanagi, H.; Shimizu, Y.; Hotta, S.; Suganuma, N.; Koyama, T.; Taniguchi, Y. *Adv. Mater.* **2002**, *14*, 1272.
(41) Ong, B. S.; Wu, Y. L.; Liu, P.; Gardner, S. *J. Am. Chem. Soc.* **2004**, *126*, 3378.
(42) Allared, F.; Hellberg, J.; Remonen, T. *Tetrahedron Lett.* **2002**, *43*, 1553.
(43) Li, X. C.; Sirringhaus, H.; Garnier, F.; Holmes, A. B.; Moratti, S. C.; Feeder, N.; Clegg, W.; Teat, S. J.; Friend, R. H. *J. Am. Chem. Soc.* **1998**, *120*, 2206.
(44) Sun, Y. M.; Ma, Y. Q.; Liu, Y. Q.; Lin, Y. Y.; Wang, Z. Y.; Wang, Y.; Di, C. A.; Xiao, K.; Chen, X. M.; Qiu, W. F.; Zhang, B.; Yu, G.; Hu, W. P.; Zhu, D. B. *Adv. Funct. Mater.* **2006**, *16*, 426.
(45) Sun, Y. M.; Liu, Y. Q.; Ma, Y. Q.; Di, C. A.; Wang, Y.; Wu, W. P.; Yu, G.; Hu, W. P.; Zhu, D. B. *Appl. Phys. Lett.* **2006**, *88*, 242113.
(46) Ponomarenko, S. A.; Kirchmeyer, S.; Elschner, A.; Huisman, B.-H.; Karbach, A.; Drechsler, D. *Adv. Funct. Mater*. **2003**, *13*, 591.
(47) Pei, J.; Wang, J. L.; Cao, X. Y.; Zhou, X. H.; Zhang, W. B.; *J. Am. Chem. Soc.* **2003**, *125*, 9944.
(48) Sun, Y. M.; Xiao, K.; Liu, Y. Q.; Wang, J. L.; Pei, J.; Yu, G.; Zhu. D. B. *Adv. Funct. Mater*. **2005**, *15*, 818.
(49) Shirota, Y. *J. Mater. Chem.* **2000**, *10*, 1.
(50) Shirota, Y. *J. Mater. Chem.* **2005**, *15*, 75.
(51) Cravino, A.; Roquet, S.; Aleveque, O.; Leriche, P.; Frere, P.; Roncali, J. *Chem. Mater.* **2006**, *18*, 2584.
(52) Saragi, T. P. I.; Lieker, T. F.; Salbeck, J. *Adv. Funct. Mater*. **2006**, *16*, 966.
(53) Saragi, T. P. I.; Lieker, T. F.; Salbeck, J. *Synth. Met.* **2005**, *148*, 267.
(54) Sonntag, M.; Kreger, K.; Hanft, D.; Strohriegl, P.; Setayesh, S.; de Leeuw, D. *Chem. Mater.* **2005**, *17*, 3031.
(55) Veres, J.; Ogier, S. D.; Leeming, S. W.; Cupertino, D. C.; Mohialdin-Khaffaf, S. *Adv. Funct. Mater.* **2003**, *13*, 199.
(56) Veres, J.; Ogier, S.; Lloyd, G. *Chem. Mater.* **2004**, *16*, 4543.
(57) Song, Y. B.; Di, C. A.; Yang, X. D.; Li, S. P.; Xu, W.; Liu, Y. Q.; Yang, L. M.; Shui, Z. G.; Zhang, D. Q.; Zhu, D. B. *J. Am. Chem. Soc.* **2006**, *128*, 15940.
(58) Xu, H.; Yu, G.; Xu, W.; Xu, Y.; Cui, G. L.; Zhang, D. Q.; Liu, Y. Q.; Zhu, D. B. *Langmuir* **2005**, *21*, 5391.
(59) Bao, Z. N.; Lovinger, A. J.; Dodabalapur, A. *Appl. Phys. Lett.* **1996**, *69*, 3066.
(60) de Boer, R. W. I.; Stassen, A. F.; Craciun, M. F.; Mulder, C. L.; Molinari, A.; Rogge, S.; Morpurgo, A. F. *Appl. Phys. Lett.* **2005**, *86*, 262109.
(61) Bao, Z. N.; Lovinger, A. J.; Brown, J. *J. Am. Chem. Soc.* **1998**, *120*, 207.
(62) Xiao, K.; Liu, Y. Q.; Huang, X. B.; Xu, Y.; Yu, G.; Zhu, D. B. *J. Phys. Chem. B.* **2003**, *107*, 9226.
(63) Su, W.; Jiang, J. Z.; Xiao, K.; Chen, Y. L.; Zhao, Q. Q.; Yu, G.; Liu, Y. Q. *Langmuir* **2005**, *21*, 6527.
(64) Chen, Y. L.; Su, W.; Bai, M.; Jiang, J. Z.; Li, X. Y.; Liu, Y. Q.; Wang, L. X.; Wang, S. Q. *J. Am. Chem. Soc.* **2005**, *127*, 15700.
(65) Wang, H.; Zhang, D.; Guo, X.; Zhu, L.; Shuai, Z.; Zhu, D. *Chem. Commun.* **2004**, 670.

(66) Wang, Y.; Wang, H. M.; Liu, Y. Q.; Di, C. A.; Sun, Y. M.; Wu, W. P.; Yu, G.; Zhang, D. Q.; Zhu, D. B. *J. Am. Chem. Soc.* **2006**, *128*, 13058.
(67) Ruiz, R.; Papadimitratos, A.; Mayer, A. C.; Malliaras, G. G. *Adv. Mater.* **2005**, *17*, 1795.
(68) Guo, X. F.; Myers, M.; Xiao, S. X.; Lefenfeld, M.; Steiner, R.; Tulevski, G. S.; Tang, J. Y.; Baumert, J. L.; Leibfarth, F.; Yardley, J. T.; Steigerwald, M. L.; Kim, P.; Nuckolls, C. *Proc. Natl. Acad. Sci.* **2006**, *103*, 11452.
(69) Ferraris, J.; Cowan, D. O.; Walatka, V.; Perlstein, J. J. H. *J. Am. Chem. Soc.* **1973**, *95*, 948.
(70) Iizuka, M.; Shiratori, Y.; Kuniyoshi, S.; Kudo, K.; Tanaka, K. *Appl. Surf. Sci.* **1998**, *914*, 130.
(71) Noda, B.; Katsuhara, M.; Aoyagi, I.; Mori, T.; Taguchi, T. *Chem. Lett.* **2005**, *34*, 392.
(72) Naraso; Nishida, J. I.; Ando, S.; Yamaguchi, J.; Itaka, K.; Koinuma, H.; Tada, H.; Tokito, S.; Yamashita, Y. *J. Am. Chem. Soc.* **2005**, *127*, 10142.
(73) Mas-Torrent, M.; Durkut, M.; Hadley, P.; Ribas, X.; Rovira, C. *J. Am. Chem. Soc.* **2004**, *126*, 984.
(74) Gao, X. K.; Wu, W. P.; Liu, Y. Q.; Qiu, W. F.; Sun, X. B.; Yu, G.; Zhu, D. B. *Chem. Commun.* **2006**, 2750.
(75) Gao, X. K.; Wu, W. P.; Liu, Y. Q.; Jiao, S. B.; Qiu, W. F.; Yu, G.; Wang, L. P.; Zhu, D. B. *J. Mater. Chem.* **2007**, *17*, 736.
(76) Lee, H. S.; Kim, D. H.; Cho, J. H.; Park, Y. D.; Kim, J. S.; Cho, K. *Adv. Funct. Mater.* **2006**, *16*, 1859.
(77) Cicoira, F.; Santato, C.; Dinelli, F.; Murgia, M.; Loi, M. A.; Biscarini, F.; Zamboni, R.; Heremans, P.; Muccini, M. *Adv. Funct. Mater.* **2005**, *15*, 375.
(78) Bao, Z.; Dodabalapur, A.; Lovinger, A. J. *Appl. Phys. Lett.* **1996**, *69*, 4108.
(79) Sirringhaus, H.; Tessler, N.; Friend, R. H. *Science* **1998**, *280*, 1741.
(80) Sirringhaus, H. *Adv. Mater.* **2005**, *17*, 2411.
(81) Afzali, A.; Dimitrakopoulos, C. D.; Breen, T. L. *J. Am. Chem. Soc.* **2002**, *124*, 8812.
(82) Weidkamp, K. P.; Afzali, A.; Tromp, R. M.; Hamers, R. J. *J. Am. Chem. Soc.* **2004**, *126*, 12740.
(83) Laquindanum, J. G.; Katz, H. E.; Lovinger, A. J. *J. Am. Chem. Soc.* **1998**, *120*, 664.
(84) Payne, M. M.; Parkin, S. R.; Anthony, J. E.; Kuo, C. C.; Jackson, T. N. *J. Am. Chem. Soc.* **2005**, *127*, 4986.
(85) Dickey, K. C.; Anthony, J. E.; Loo, Y. L. *Adv. Mater.* **2006**, *18*, 1721.
(86) Shklyarevskiy, I. O.; Jonkheijm, P.; Stutzmann, N.; Wasserberg, D.; Wondergem, H. J.; Christianen, P. C. M.; Schenning, A. P. H. J.; de Leeuw, D. M.; Tomovic, Z.; Wu, J.; Müllen, K.; Maan, J. C. *J. Am. Chem. Soc.* **2005**, *127*, 16233.
(87) Dimitrakopoulos, C. D.; Kymissis, I.; Purushothaman, S.; Neumayer, D. A.; Duncombe, P. R.; Laibowitz, R. B. *Adv. Mater.* **1999**, *11*, 1372. (b) Dimitrakopoulos, C. D.; Purushothaman, S.; Kymissis, J.; Callegari, A.; Shaw, J. M. *Science* **1999**, *283*, 822.
(88) Yuan, J. F.; Zhang, J.; Wang, J.; Yan, X. J.; Yan, D. H.; Xu, W. *Appl. Phys. Lett.* **2003**, *82*, 3967.
(89) Peng, X.; Horowitz, G.; Fichou, D.; Garnier, F. *Appl. Phys. Lett.* **1990**, *57*, 2013.
(90) Bao, Z.; Feng, Y.; Dodabalapur, A.; Raju, V. R.; Lovinger, A. J. *Chem. Mater.* **1997**, *9*, 1299.
(91) Halik, M.; Klauk, H.; Zschieschang, U.; Schmid, G.; Dehm, C.; Schutz, M.; Maisch, S.; Effenberger, F.; Brunnbauer, M.; Stellacci, F. *Nature* **2004**, *431*, 963.
(92) Facchetti, A.; Yoon, M. H.; Marks, T. J. *Adv. Mater.* **2005**, *17*, 1705.
(93) Yoon, M. H.; Kim, C.; Facchetti, A.; Marks, T. J. *J. Am. Chem. Soc.* **2006**, *128*, 12851.
(94) Ahles, M.; Schmechel, R.; Seggern, H. V. *Appl. Phys. Lett.* **2004**, *85*, 4499.
(95) Chua, L. L.; Zaumseil, J.; Chang, J. F.; Ou, E. C. W.; Ho, P. K. H.; Sirringhaus, H.; Friend, R. H. *Nature* **2005**, *434*, 194.
(96) Baeg, K. J.; Noh, Y. Y.; Ghim, J.; Kang, S. J.; Lee, H.; Kim, D. Y. *Adv. Mater.* **2006**, *18*, 3179.
(97) Yasuda, T.; Tsutsui, T. *Chem. Phys. Lett.* **2005**, *402*, 395.
(98) Takahashi, T.; Takenobu, T.; Takeya, J.; Iwasa, Y. *Appl. Phys. Lett.* **2006**, *88*, 033505.
(99) Anthopoulos, T. D.; Setayesh, S.; Smits, E.; Cölle, M.; Cantatore, E.; de Boer, B.; Blom, P. W. M.; de Leeuw, D. M. *Adv. Mater.* **2006**, *18*, 1900.
(100) Watkins, N. J.; Yan, L.; Gao, Y. L. *Appl. Phys. Lett.* **2002**, *80*, 4384.
(101) Cho, J. H.; Kim, D. H.; Jang, Y.; Lee, W. H.; Ihm, K.; Han, J.; Chung, S.; Cho, K. *Appl. Phys. Lett.* **2006**, *89*, 132101.
(102) Hajlaoui, R.; Horowitz, G.; Garnier. F.; Brouchet, A. A.; Laigre, L.; Kassmi, A. E.; Demanze, F.; Kouki, F. *Adv. Mater.* **1997**, *9*, 389.
(103) Chu, C. W.; Li, S. H.; Chen, C. W.; Shrotriya, V.; Yang, Y. *Appl. Phys. Lett.* **2005**, *87*, 193508.
(104) Kymissis, I.; Dimitrakopoulos, C. D.; Purushothaman, S. *IEEE Trans. Electron Devices* **2001**, *48*, 1060.
(105) Gundlach, D. J.; Jia, L. L.; Jackson, T. N. *IEEE Electron Device Lett.* **2001**, *22*, 571.
(106) Koch, N.; Elschner, A.; Rabe, J. P.; Johnson, R. L. *Adv. Mater.* **2005**, *17*, 330.
(107) Cao, Q.; Hur, S. H.; Zhu, Z. T.; Sun, Y. G.; Wang, C. J.; Meitl, M. A.; Shim, M.; Rogers, J. A. *Adv. Mater.* **2006**, *18*, 304.
(108) Luan, S.; Neudeck, G. W. *J. Appl. Phys.* **1992**, *72*, 766.
(109) Lefenfeld, M.; Blanchet, G.; Rogers, J. A. *Adv. Mater.* **2003**, *15*, 1188.
(110) Jurchescu, O. D.; Popinciuc, M.; van Wees, B. J.; Palstra, T. T. M. *Adv. Mater.* **2007**, *19*, 688.
(111) Sundar, V. C.; Zaumseil, J.; Podzorov, V.; Menard, E.; Willett, R. L.; Someya, T.; Gershenson, M. E.; Rogers, J. A. *Science* **2004**, *303*, 1644.
(112) Zeis, R.; Siegrist, T.; Kloc, Ch. *Appl. Phys. Lett.* **2005**, *86*, 022103.
(113) Menard, E.; Podzorov, V.; Hur, S. H.; Gaur, A.; Gershenson, M. E.; Rogers, J. A. *Adv. Mater.* **2004**, *16*, 2097.
(114) Goldmann, C.; Haas, S.; Krellner, C.; Pernstich, K. P.; Gundlach, D. J.; Batlogg, B. *J. Appl. Phys.* **2004**, *96*, 2080.
(115) Podzorov, V.; Sysoev, S. E.; Loginova, E.; Pudalov, V. M.; Gershenson, M. E. *Appl. Phys. Lett.* **2003**, *83*, 3504.
(116) Briseno, A. L.; Tseng, R. J.; Ling, M. M.; Falcao, E. H. L.; Yang, Y.; Wudl, F.; Bao, Z. N. *Adv. Mater.* **2006**, *18*, 2320.
(117) Tang, Q. X.; Li, H. X.; Liu, Y. L.; Hu, W. P. *J. Am. Chem. Soc.* **2006**, *128*, 14634.
(118) Tang, Q. X.; Li, H. X.; Song, Y. B.; Xu, W.; Hu, W. P.; Jiang, L.; Liu, Y. Q.; Wang, X. K.; Zhu, D. B. *Adv. Mater.* **2006**, *18*, 3010.
(119) Sun, Y. M.; Tan, L.; Jiang, S. D.; Qian, H. L.; Wang, Z. H.; Yan, D. W.; Di, C. A.; Wang, Y.; Wu, W. P.; Yu, G.; Yan, S. K.; Wang, C. R.; Hu, W. P.; Liu, Y. Q.; Zhu, D. B. *J. Am. Chem. Soc.* **2007**, *129*, 1882.
(120) Briseno, A. L.; Miao, Q.; Ling, M. M.; Reese, C.; Meng, H.; Bao, Z. N.; Wudl, F. *J. Am. Chem. Soc.* **2006**, *128*, 15576.
(121) Yanagi, H.; Morikawa, T.; Hotta, S.; Yase, K. *Adv. Mater.* **2001**, *13*, 313.
(122) Ichikawa, M.; Yanagi, H.; Shimizu, Y.; Hotta, S.; Suganuma, N.; Koyama, T.; Taniguchi, Y. *Adv. Mater.* **2002**, *14*, 1272.
(123) Wilkinson, F. S.; Norwood, R. F.; McLellan, J. M.; Lawson, L. R.; Patrick, D. L. *J. Am. Chem. Soc.* **2006**, *128*, 16468.
(124) Briseno, A. L.; Mannsfeld, S. C. B.; Ling, M. M.; Liu, S. H.; Tseng, R. J.; Reese, C.; Roberts, M. E.; Yang, Y.; Wudl, F.; Bao, Z. N. *Nature* **2006**, *444*, 913.